Peptidomimetics

Using a β-Hairpin To Mimic an α-Helix: Cyclic Peptidomimetic Inhibitors of the p53–HDM2 Protein–Protein Interaction**

*Rudi Fasan, Ricardo L. A. Dias, Kerstin Moehle, Oliver Zerbe, Jan W. Vrijbloed, Daniel Obrecht, and John A. Robinson**

The design of novel protein ligands and inhibitors of protein–protein interactions is an important goal in post-genomic proteome analyses and in drug and vaccine discovery. Unfortunately, the design of synthetic molecules that target surface-exposed regions on folded proteins is presently difficult. Moreover, typical libraries of small "druglike" compounds have so far not been a fruitful source of protein–protein interaction inhibitors. One potential approach to such inhibitors arises through the design and synthesis of peptidomimetics that reproduce the conformational and electronic properties of functional native protein epitopes (so-called protein epitope mimetics (PEMs)). One supersecondary structure frequently found at natural protein–protein interfaces is the β-hairpin motif. Conceivably, β-hairpin mimetics, just like the natural motifs in functional protein epitopes, may provide a robust presentation platform upon which the groups (e.g. side chains) essential for protein surface capture can be combined in a structurally defined yet malleable array. As an illustration of this approach and the robustness of the β-hairpin scaffold, we show here how β-hairpin PEMs based on a naturally occurring α-helical peptide can be designed as inhibitors of the p53–HDM2 interaction.

The p53 tumor suppressor, which is present at low concentrations in normal cells and at elevated levels in cells subject to stress, is regulated by its interaction with HDM2. The design of molecules that inhibit the interaction between p53 and HDM2 appears to be an attractive strategy for increasing p53 tumor-suppressor activity in tumor cells.[1] The HDM2-binding domain on p53 is localized to a region at the N-terminus of the protein, from about residues 10–30. The p53-binding domain on HDM2 is also located at the N-terminus of this multidomain protein from residues 1–120. The structure of a complex formed between HDM2 (residues 17–125) and a p53-derived peptide (residues 15–29) has been determined by X-ray crystallography.[2] The p53-derived peptide adopts a largely amphipathic α-helical backbone conformation, with the side chains of Phe19, Trp23, and Leu26 inserting into hydrophobic pockets on the surface of the HDM2 domain (Figure 1). The HDM2–p53 interface buries a total of 1498 Å^2 of surface in the complex, or about 690 Å^2 and 808 Å^2, respectively, on each protein. Some of the few known p53–HDM2 inhibitors include the natural product chlorofusin,[3,4] various linear peptides,[5–13] and some chalcone derivatives.[14]

For the design of a p53 mimetic we noted that the distance between the C_α atoms of Phe19 and Trp23 on one face of the HDM2-bound p53 α-helix is close to the distance expected between the C_α atoms of two residues i and $i+2$ along one strand of a β-hairpin (see Figure 2). A designed hairpin

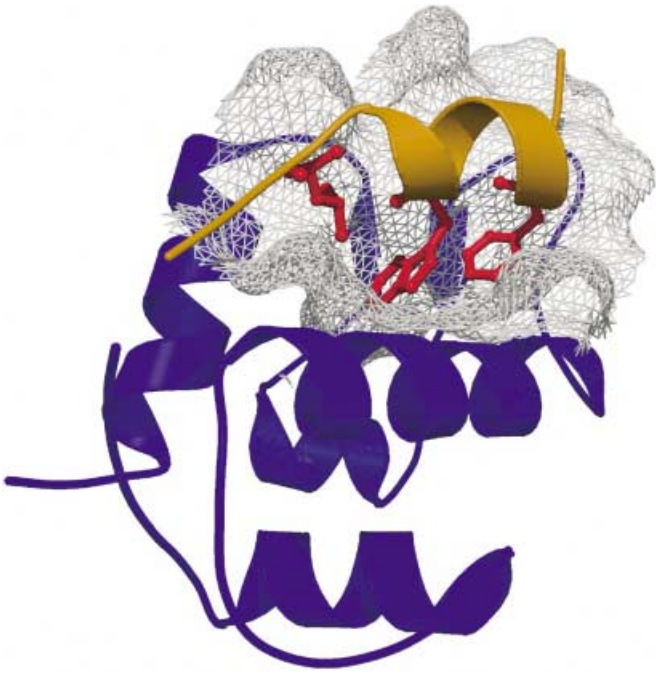

Figure 1. Ribbon and surface representation of the crystal structure of the complex consisting of a p53-derived peptide (yellow) and HDM2 (blue).[2] The side chains of Leu26, Trp23, and Phe19 in p53 are highlighted in red. The representation was prepared using Molscript,[23] Grasp,[24] and Raster 3D.[25]

Figure 2. A model β-hairpin (yellow) superimposed on the p53 helical peptide (red, see text and Figure 1). The β-hairpin could act as a scaffold to preorganize side chains to give a geometry similar to that seen in a helical peptide.

[*] R. Fasan, Dr. R. L. A. Dias, Dr. K. Moehle, Dr. O. Zerbe, Prof. J. A. Robinson
Institute of Organic Chemistry
University of Zürich
Winterthurerstrasse 190, 8057 Zürich (Switzerland)
Fax: (+41) 1-635-6833
E-mail: robinson@oci.unizh.ch
Dr. J. W. Vrijbloed, Dr. D. Obrecht
Polyphor AG
Gewerbestrasse 14, 4123-Allschwil (Switzerland)

[**] The authors thank the Swiss National Science Foundation for financial support and Dr. Heiko Henze and Annelies Meier for technical support.

 DOI: 10.1002/anie.200353242

mimetic could therefore function as a scaffold to hold the side chains of Phe 19 and Trp 23 (and possibly also Leu 26) in the correct relative positions so that each can interact simultaneously with the p53 binding site on HDM2.

To test this idea, the hairpin mimetic **1** was designed, in which an eight-residue loop is preorganized into a regular β-hairpin by mounting upon a D-Pro-L-Pro dipeptide template. We have described in earlier work how D-Pro-L-Pro can function as a template to stabilize β-hairpin loop conformations in cyclic mimetics.[15–19] In a computer model of **1**, the residues Phe 1, Trp 3, and Leu 4 appear ideally placed to mimic the critical residues Phe 19, Trp 23, and Leu 26 in p53 (Figure 2). Mimetic **1** was synthesized on 2-chlorotrityl chloride resin as shown in Scheme 1 and purified by reverse-phase HPLC.

A BIAcore (Biacore AB) solution-phase competition assay was used to monitor binding of the mimetic **1** to HDM2. The biotin-SGSG-p53 (residues 15–29) peptide conjugate **2** was immobilized on a streptavidin-coated biosensor chip. The HDM2 protein (residues 17–126) with a His_6-tag fused to the N-terminus, was produced in *E. coli* using the vector pET14b (Novagen). This protein binds to the p53 peptide–sensor surface with a $K_d = 670$ nM (cf. $K_d =$ 600 nM for a peptide corresponding to residues 15–29 of p53[2]). The affinity of mimetics to HDM2 could then be expressed as an IC_{50} value, by coinjecting each with HDM2 (250 nM, in HEPES buffer (10 mM, pH 7.4) with NaCl (150 mM), EDTA (3.4 mM) and surfactant p20 (0.005% v/v)) over the biosensor surface. With increasing concentrations of the mimetic, the binding of HDM2 to the surface is increasingly inhibited, which leads to a decrease in the biosensor response (see Table 1 and Figure 3). In this way, the IC_{50} value for the linear p53-derived peptide **3** was determined to be 1.1 μM. Although the affinity of **1** for HDM2 appears weak ($IC_{50} = 125$ μM), it provided a lead for optimization.

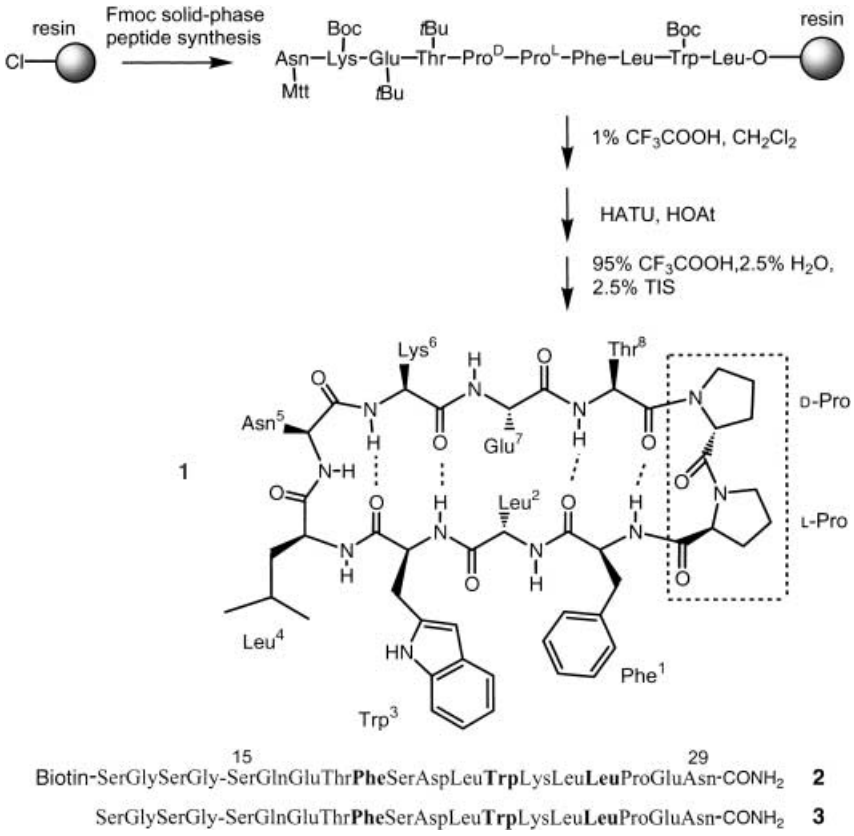

Scheme 1. Synthesis of mimetic **1**. HATU = 2-(1-hydroxy-7-azabenzotriazol-1-yl)-1,1,3,3-tetramethyluronium hexafluorophosphate, HOAt = 1-hydroxy-7-azabenzotriazole, TIS = triisopropylsilyl.

Table 1: The inhibitory concentrations of peptidomimetics causing a 50% drop in biosensor response (IC_{50} μM) in the BIAcore assay (see text and Figure 3). Positions 1–8 refer to the residues 1–8, mounted on the D-Pro-L-Pro template (as shown for **1** in Scheme 1).

Mimetic	Position								IC_{50} [μM][a]
	1	2	3	4	5	6	7	8	
1	F	L	W	L	N	K	E	T	125 ± 8
4	F	L	W	A	N	K	E	T	350 ± 6
5	F	L	A	L	N	K	E	T	> 1000
6	F	A	W	L	N	K	E	T	207 ± 15
7	A	L	W	L	N	K	E	T	> 1000
8	F	L	W	L	N	K	E	A	122 ± 10
9	F	L	W	L	N	K	A	T	195 ± 7
10	F	L	W	L	N	A	E	T	650 ± 35
11	F	L	W	L	A	K	E	T	250 ± 6
12	F	L	W	L	N	Y	E	T	53 ± 2
13	F	K	W	L	N	Y	E	F	9.5 ± 2.4
14	F	E	W	L	N	W	E	Y	1.4 ± 0.3
15	F	E	W	L	N	W	E	F	0.89 ± 0.05
16	F	E	W	L	D	W	E	F	0.53 ± 0.06
17	F	E	W	L_N[b]	N	F	E	Y	2.6 ± 0.6
18	F	E	W	L_N[b]	D	W	E	F	0.37 ± 0.07
19	F	E	(6Cl)-W[b]	L	D	W	E	F	0.14 ± 0.06

[a] Mean value and standard deviation result from at least three independent experiments. [b] The usual symbols for proteinogenic amino acids are used, except L_N refers to *N*-(2-methylpropyl)-glycine and (6-Cl)W refers to 6-chlorotryptophan.

A library of eight mimetics (**4**–**11**), in which each residue in **1** was replaced by alanine, was made and tested. This revealed that not only the side chains of Phe 1, Trp 3, and

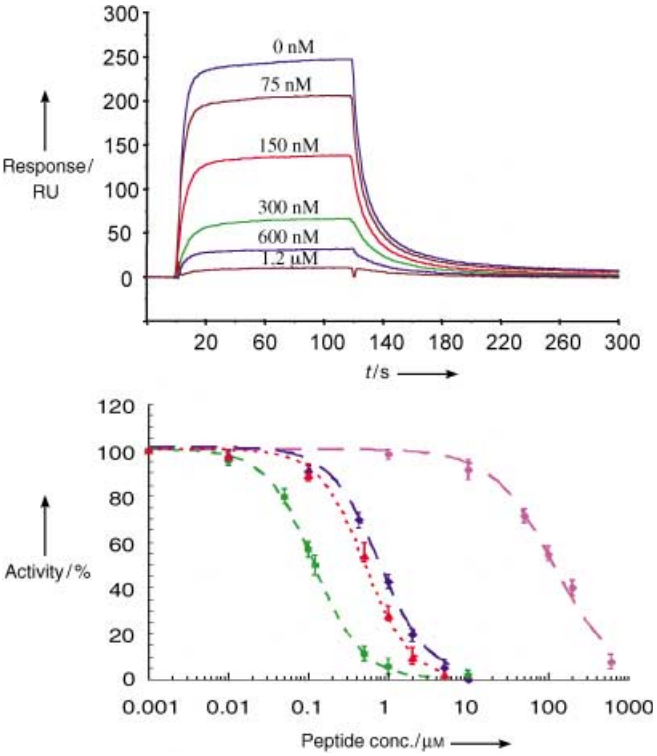

Figure 3. Top: Sensorgrams from the BIAcore inhibition assay (see text), showing the decrease in response upon addition of increasing amounts of peptidomimetic **19** (see Table 1). Bottom: The BIAcore data for mimetics **1** (magenta), **15** (blue), **16** (red), and **19** (green) as used to derive IC_{50} values (see Table 1).

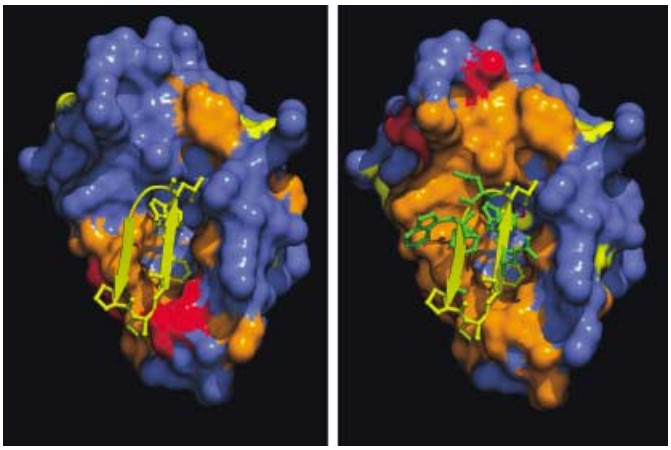

Figure 4. Surface representations of HDM2 illustrating the locations of residues that experience changes in [^{15}N,^{1}H]-HSQC spectra upon addition of the peptidomimetic **1** (left) and **19** (right) to U-^{15}N-labeled HDM2. The hairpin mimetics shown have been modeled (Figure 2) into the p53 binding site on HDM2 by docking/energy minimization. Red = chemical shift $\Delta\delta > 0.22$ ppm, yellow = $\Delta\delta = 0.22$–0.15 ppm, orange = much reduced intensity of cross-peak in 2D spectrum, blue = no change (where $\Delta\delta = \sqrt{(\Delta\delta^{1}H)^2 + (0.2\,\Delta\delta^{15}N)^2}$). The representation was prepared using Molscript,[23] Grasp,[24] and Raster 3D.[25]

Leu4 (as expected), but also that of Lys6 make important energetic contributions to HDM2 binding (see Table 1). Further libraries, in which individual residues in **1** were exchanged for other proteinogenic amino acids, were then prepared and screened. For example, a K6Y replacement (**12**) improved the IC_{50} to 53 μM; mimetic **13** with three changes has an IC_{50} value of 9.5 μM; derivative **14** has an IC_{50} value close to that seen for the p53-derived peptide **3**; whereas mimetics **15** and **16** are submicromolar inhibitors. Further mimetics were also prepared containing non-proteinogenic amino acid building blocks. The derivatives **17** and **18** have a peptoid unit at the hairpin tip, and **19** has a 6-chlorotryptophan at position 3. This last mimetic displays an increase in affinity for HDM2 over that of the initial lead **1** by a factor of almost 900-fold, and an improvement over that of the linear p53 analogue **3** by almost 8-fold. Another comparison is with the natural product chlorofusin, itself a cyclic peptide, whose IC_{50} value determined by ELISA was 4.6 μM.[3]

Evidence that the mimetics interact with HDM2 at the p53 binding site was obtained by NMR spectroscopy. 2D [^{15}N,^{1}H]-HSQC spectra of uniformly ^{15}N-labeled HDM2 were recorded in the presence and absence of mimetic. Using NMR assignments reported earlier,[14] the site contacted by **1** and **19** on HDM2 was mapped by measuring changes in chemical shifts of backbone H^{N}-N^{15} cross-peaks upon binding. The largest changes occurred for residues within and around the p53 binding site revealed by crystallography (Figure 4), although several perturbations are more remote from the interaction site, possibly due to changes in protein conformation that are required to accommodate the ligand. Whereas **1** appeared to be in fast exchange between the HDM2-bound and free states, on the chemical shift time-scale, the bound form of mimetic **19** was shown to be in slow exchange with the free form, as evident from the occurrence of two sets of cross-peaks for substoichiometric concentrations of **19**.

The solution structures of several mimetics have also been investigated by NMR spectroscopy in 1:1 MeOH/water (the peptides are not sufficiently soluble for studies in pure water). For example, average NMR structures were determined for mimetic **17** in solution (1:1 CD_3OD:H_2O/D_2O (9/1), pH(apparent) 5, 300 K), using NOE-derived upper-distance limits as restraints with DYANA[20] (see Table 2). It was apparent from the numerous cross-hairpin connectivities seen in NOESY spectra that this molecule adopts a regular β-hairpin conformation (see Figure 5), with a β-turn at the hairpin tip. A

Table 2: Summary of conformational constraints and statistics for the NMR structure calculations performed on mimetic **17** with the program DYANA. The final 20 NMR structures are shown in Figure 5.

	Mimetic **17**
NOE upper-distance limits	76
Intraresidue	22
Sequential	33
Medium- and long-range	21
Dihedral angle restraints (HN-C_α-H)	7
Residual target function value	0.53 ± 0.18 Å^2
Mean RMSD values	
All backbone atoms	0.53 ± 0.31 Å^2
All heavy atoms	1.66 ± 0.34 Å^2
Residual NOE violations	
Number > 0.2 Å	8
Maximum	0.35 Å^2

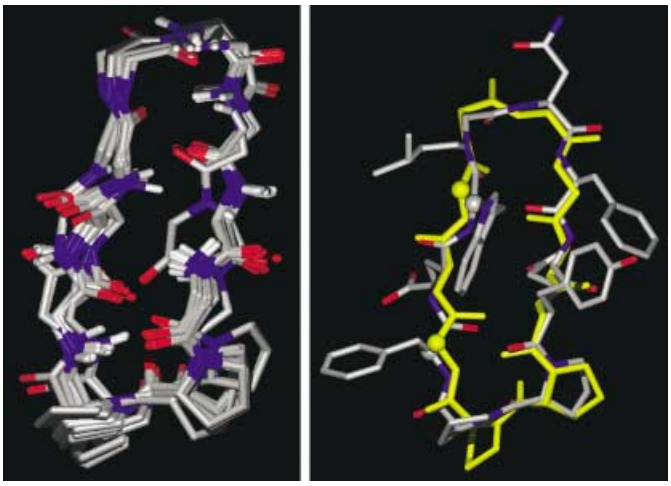

Figure 5. Left: Superimposition of the backbone atoms in 20 DYANA[20] structures (ave root mean square distance for all backbone atoms to mean: 0.53 Å; see Table 2) of mimetic **17** after optimization with GROMOS.[26] The D-Pro-L-Pro template is at the bottom. N = blue, O = red; side chains omitted for clarity. Right: Superposition of one typical NMR structure of **17** and the starting β-hairpin model peptide (in yellow), as shown in Figure 2. The representation was prepared using Molmol.[27]

superposition of one typical NMR structure with the β-hairpin model used at the outset and depicted in Figure 2 is shown in Figure 5. It is also noteworthy that an increase in amphiphilicity of the β-hairpin parallels the improved affinity as **1** is changed to **17** (see also **12**–**19**). An extensive aromatic core is thereby generated on one face, which may both stabilize the hairpin structure through cross-strand aromatic interactions,[21,22] and promote association with the rather hydrophobic p53-binding site on HDM2.[2] Work is now ongoing to determine the structure(s) of the bound forms of these inhibitors and to investigate the mechanism(s) of binding in more detail.

In conclusion, the structural data together with the functional binding data provide confirmation of our starting hypothesis, that a β-hairpin can be used to mimic some features of an α-helical peptide. This type of mimicry may be of general use in the design of other novel PEM-based inhibitors of protein–protein interactions. Moreover, the mimetics reported here might be of direct value in the search for novel agents with tumor-suppressor activity.

Received: November 4, 2003 [Z53242]

Keywords: antitumor agents · inhibitors · peptidomimetics · protein structures

[1] P. Chéne, *Nat. Rev. Cancer* **2003**, *3*, 102.
[2] P. H. Kussie, S. Gorina, V. Marechal, B. Elenbaas, J. Moreau, A. J. Levine, N. P. Pavletich, *Science* **1996**, *274*, 948.
[3] S. J. Duncan, S. Grüschow, D. H. Williams, C. McNicholas, R. Purewal, M. Hajek, M. Gerlitz, S. Martin, S. K. Wrigley, M. Moore, *J. Am. Chem. Soc.* **2001**, *123*, 554.
[4] S. J. Duncan, M. A. Cooper, D. H. Williams, *Chem. Commun.* **2003**, 316.
[5] R. Banerjee, G. Basu, P. Chéne, S. Roy, *J. Pept. Res.* **2002**, *60*, 88.
[6] C. Garcia-Echeverria, C. P. , M. J. J. Blommers, P. Furet, *J. Med. Chem.* **2000**, *43*, 3205.
[7] C. Garcia-Echeverria, P. Furet, P. Chéne, *Bioorg. Med. Chem. Lett.* **2001**, *11*, 2161.
[8] P. Chéne, J. Fuchs, J. Bohn, C. Garcia-Echeverria, P. Furet, D. Fabbro, *J. Mol. Biol.* **2000**, *299*, 245.
[9] V. Böttger, A. Böttger, S. F. Howard, S. M. Picksley, P. Chéne, C. Garcia-Echeverria, H.-K. Hochkeppel, D. P. Lane, *Oncogene* **1996**, *13*, 2141.
[10] A. Böttger, V. Böttger, A. Sparks, W.-L. Liu, S. F. Howard, D. P. Lane, *Curr. Biol.* **1997**, *7*, 860.
[11] M. Kanovsky, A. Raffo, L. Drew, R. Rosal, T. Do, F. K. Friedman, P. Rubinstein, J. Visser, R. Robinson, P. W. Brandt-Rauf, J. Michl, R. L. Fine, M. R. Pincus, *Proc. Natl. Acad. Sci. USA* **2001**, *98*, 12438.
[12] S. M. G. Knight, N. Umezawa, H.-S. Lee, S. H. Gellman, B. K. Kay, *Anal. Biochem.* **2002**, *300*, 230.
[13] V. J. Huber, T. W. Arroll, C. Lum, B. A. Goodman, H. Nakanishi, *Tetrahedron Lett.* **2002**, *43*, 6729.
[14] R. Stoll, C. Renner, S. Hansen, S. Palme, C. Klein, A. Belling, W. Zeslawski, M. Kamionka, T. Rehm, P. Mühlhahn, R. Schumacher, F. Hesse, B. Kaluza, W. Voelter, R. A. Engh, T. A. Holak, *Biochemistry* **2001**, *40*, 336.
[15] L. Jiang, K. Moehle, B. Dhanapal, D. Obrecht, J. A. Robinson, *Helv. Chim. Acta* **2000**, *83*, 3097.
[16] M. Favre, K. Moehle, L. Jiang, B. Pfeiffer, J. A. Robinson, *J. Am. Chem. Soc.* **1999**, *121*, 2679.
[17] A. Descours, K. Moehle, A. Renard, J. A. Robinson, *ChemBioChem* **2002**, *3*, 318.
[18] S. C. Shankaramma, Z. Athanassiou, O. Zerbe, K. Moehle, C. Mouton, F. Bernardini, J. W. Vrijbloed, D. Obrecht, J. A. Robinson, *ChemBioChem* **2002**, *3*, 1126.
[19] S. C. Shankaramma, K. Moehle, S. James, J. W. Vrijbloed, D. Obrecht, J. A. Robinson, *Chem. Commun.* **2003**, 1842.
[20] P. Güntert, C. Mumenthaler, K. Wüthrich, *J. Mol. Biol.* **1997**, *273*, 283.
[21] S. J. Russell, A. G. Cochran, *J. Am. Chem. Soc.* **2000**, *122*, 12600.
[22] C. D. Tatko, M. L. Waters, *J. Am. Chem. Soc.* **2002**, *124*, 9372.
[23] P. J. Kraulis, *J. Appl. Crystallogr.* **1991**, *24*, 946.
[24] A. Nicholls, K. Sharp, B. Honig, *Proteins Struct. Funct. Genet.* **1991**, *11*, 281.
[25] E. A. Merritt, D. J. Bacon, *Methods Enzymol.* **1997**, *277*, 505.
[26] W. F. van Gunsteren, S. R. Billeter, A. A. Eising, P. H. Hünenberger, P. Krüger, A. E. Mark, W. R. P. Scott, I. G. Tironi, *Biomolecular Simulation: The GROMOS96 Manual and User Guide*, Hochschulverlag AG an der ETH Zürich, Zurich, **1996**.
[27] R. Koradi, M. Billeter, K. Wüthrich, *J. Mol. Graphics* **1996**, *14*, 51.

